Progress In Electromagnetics Research M, Vol. 33, 169–183, 2013

FREQUENCY DEPENDENT CHARACTERISTICS OF GROUNDING SYSTEM BURIED IN MULTILAYERED EARTH MODEL BASED ON QUASI-STATIC ELECTROMAGNETIC FIELD THEORY

Zhong-Xin Li*, Yu Yin, Cui-Xia Zhang, and Liu-Cun Zhang

China Electric Power Research Institute, No. 15, East Road, Xiaoying, Qinghe, Haidian, Beijing, China

Abstract—The frequency dependent characteristics of grounding system buried in half homogenous earth model have been discussed before; however, the importance of mutual inductive and capacitive effects on the grounding problems in both frequency and time domains is unclear. In order to study the importance of the mutual inductive, capacitative and conductive effects on the grounding problem in both frequency and time domains, hybrid method, which is a hybrid of Galerkin's method of moment and conventional nodal analysis method, has been used to study the dominant factor among the mutual inductive, capacitive and conductive effects in the paper.

1. INTRODUCTION

The frequency dependent characteristics of grounding system have been discussed in papers [1] and [2] considering mutual inductive and capacitive effects; however, only uniform earth model is considered. Recently, paper [3] discussed the characteristics of grounding impedance of grounding system in frequency domain without considering mutual capacitive effect. Paper [4] discussed the characteristics of grounding impedance of grounding systems in both the frequency and time domain with mutual inductive and capacitive effects neglected. Paper [5] studied the high frequency characteristics of grounding impedance with mutual inductive effect neglected. Paper [6] discussed the characteristics of impulse grounding impedance of grounding systems in the time domain with mutual capacitive effect neglected. It should be pointed out that all these

Received 19 August 2013, Accepted 11 October 2013, Scheduled 17 October 2013

* Corresponding author: Zhong Xin Li (zxli@fudan.edu.cn).

grounding systems were buried in only half homogenous earth model. Meanwhile, the importance of mutual inductive and capacitive effects on the grounding problems in both frequency and time domains is unclear. In order to study the importance of the mutual inductive, capacitative and conductive effects on the grounding problem in both frequency and time domains, hybrid method developed in papers [29–32, 34] has been used.

It must be pointed out that computerized analysis methods have been developed based on different approaches, for example, circuit theory [6–9], transmission line theory [10–16], electromagnetic field theory [1, 17–26], and hybrid methods [3, 27–34]. The hybrid method has been developed from conventional nodal analysis method [35], which combines electric circuit method and electromagnetic field method, and has been proved to have strong-points of both the methods.

In this paper, based on the hybrid method developed in paper [34], frequency dependent characteristics of grounding systems buried in an horizontal multilayered earth model have been discussed. The frequency dependent characteristics of grounding systems buried in the horizontal multilayered earth model have been studied due to neglecting mutual inductive effect, mutual capacitive effect or both of them by using different parameters of the earth model.

2. HYBRID METHOD MATHEMATICAL MODEL OF EQUIVALENT CIRCUIT OF THE GROUNDING SYSTEM IN FREQUENCY DOMAIN

The transient problem is first solved by a formulation in the frequency domain. The response to a steady state, time harmonic excitation, is computed for a wide range of frequencies starting at zero Hz. The time-domain response is then obtained by application of a suitable Fourier inversion technique [20].

A set of interconnected cylindrical thin conductors placed in any position or orientation consists of a network to form a grounding system. The grounding network's conductors are assumed to be completely buried in an horizontal multilayered earth. The methodology proposed is based on the study of all the inductive, capacitive and conductive couplings between different conductors of the grounding system. The grounding system can be divided into N_l pieces of segments and owns N_p discrete nodes, and each of them can be studied as an elemental unit.

According to papers [2, 4, 33, 34], the obtained electric circuit may be studied using the conventional nodal analysis method [35], resulting

in the following equations:

$$[\overline{\mathbf{F}}] = [\overline{\overline{\mathbf{Y}}}] \cdot [\overline{\mathbf{V_n}}] \tag{1}$$

$$[\overline{\overline{\mathbf{Y}}}] = [\overline{\overline{\mathbf{K}}}]^t \cdot [\overline{\overline{\mathbf{Z_S}}}]^{-1} \cdot [\overline{\overline{\mathbf{K}}}] + [\overline{\overline{\mathbf{A}}}] \cdot [\overline{\overline{\mathbf{Z_b}}}]^{-1} \cdot [\overline{\overline{\mathbf{A}}}]^t \tag{2}$$

where $[\overline{\mathbf{F}}]$ is a $N_p \times 1$ vector of external current sources; $[\overline{\overline{\mathbf{Z}_b}}]$ or $[\overline{\overline{\mathbf{Z_S}}}]$, are, respectively, the $N_l \times N_l$ mutual induction or impedance matrices of the circuit of grounding system, which include resistive and inductive or capacitive and conductive effects of a pairs of short conducts buried in an horizontal multilayered earth. Both $[\overline{\overline{\mathbf{A}}}]$ and $[\overline{\overline{\mathbf{K}}}]$ are incidence matrices, which are used to relate to branches and nodes. There are rectangular matrices of order $N_l \times N_p$, whose elements can refer to papers [2, 4, 33, 34].

The vector of nodal SEP $[\overline{\mathbf{V_n}}]$ may be calculated by solving Eq. (1). Further, the average SEP $[\overline{\mathbf{U}}]$, leakage currents, branch voltage, and branch current can also be calculated. Meanwhile, the SEP at any point can be calculated, ans all these calculations can refer to papers [2, 4, 33 34].

The study of the grounding systems performance in frequency domain has been reduced to the computation of $[\overline{\overline{\mathbf{Z_S}}}]$ and $[\overline{\overline{\mathbf{Z_b}}}]$ matrices. The calculation for the elements of $[\overline{\overline{\mathbf{Z_S}}}]$ and $[\overline{\overline{\mathbf{Z_b}}}]$ matrices is about mutual induction and impedance coefficients. The formula about the mutual induction and impedance coefficients can be fast calculated with quasi-static complex image method and closed form of Green's function of a dipole and monopole adopted, which can refer to papers [29–32, 34]. The mathematical model can be used to calculate the lightning response to the grounding problem buried in the multilayered earth model through FFT, and its verification has been fully discussed in paper [34].

3. SIMULATION RESULT AND ANALYSIS

A typical grounding system can be seen in Fig. 1. Different parameters of an horizontal multilayered earth model are analyzed, which can be seen in Table 1. Three cases of parameters are given. Cases 1 and 2 can be seen in Table 1, and case 3 is the same as case 2 except that the relative permittivity value is 80 instead of 10. The material of the grounding system conductor is Cu with conductivity $\sigma_{Cu} = 5.8 \times 10^7$ S/m. The conductor radius is 7 mm. The external excited lighting current is injected from the corner of the grounding system, which is described by a double-exponential function as $I(t) = 10.416 \times (e^{-9.725\times10^{-3}t} - e^{-0.217t})$ A, which means that parameters of

Table 1. Different horizontal multilayered earth model.

No.	case 1		case 2	
	ρ_1	ρ_2	ρ_1	ρ_2
1 layer case	900.0		100.0	
2 layer case	900.0	500.0	100.0	300.0
	ϵ_1	ϵ_2	ϵ_1	ϵ_2
1 layer case	10.0		10.0	
2 layer case	10.0	10.0	10.0	10.0
	h_1	h_2	h_1	h_2
1 layer case				
2 layer case	0.6		0.6	

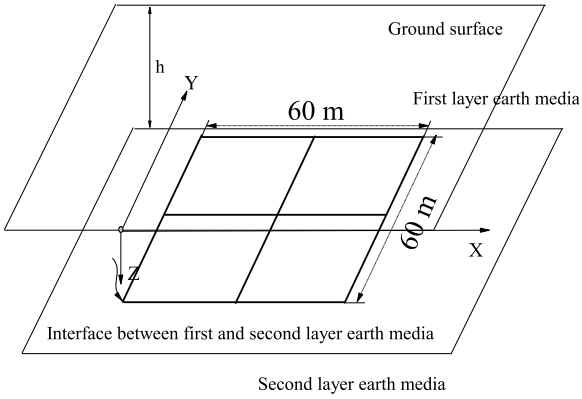

Figure 1. Typical grounding system.

the lighting current are $T_1 = 15\,\mu s$, $T_2 = 91\,\mu s$ and $I_m = 10.0\,A$. It must be pointed out that impulse impedance, an essential parameter in grounding system design, is defined by the following expression in paper [36].

3.1. 1-layer Earth Model

The transient SEP at injection point within three cases of 1-layer earth model are given in Fig. 2, and real and imaginary parts of grounding impedance within three cases of 1-layer earth model are given in Figs. 3, 4. Table 2 shows impulse impedances of the grounding system buried in the 1-layer earth model. To better illuminate later, the curves in these figures produced with mutual inductive and capacitive effects are

called original curves.

Figure 2 shows dashed curves ((a) black color, (b) red color, (c) green color, (d) blue color) of transient SEP at injection point within case 1 of 1-layer earth model. The peak value for the four curves is about 78.8 V. The resistivity of the earth is 900 Ωm, and relative permittivity is 10, which means that the mutual conductive effect is much higher. So, once mutual capacitive effect has been neglected, curve (b) of transient SEP at injection point is a superposition with the original curve (a), and once mutual inductive effect has been neglected, curve (c) of transient SEP at injection point is like original curve (a). Meanwhile, the impulse impedances of the three cases are almost same. However, once both mutual inductive and capacitive effects have been ignored. Curve (d) of transient SEP at injection point is lower than the original curve (a). The impulse impedance also becomes smaller as $(8.97, 5.33 \times 10^{-4})\,\Omega$. All these show that mutual inductive and capacitive effects are much smaller than mutual conductive effect due to high resistivity of the earth. In other words, the mutual conductive effect is dominant.

Figure 2 also shows dotted curves ((a), (b), (c), (d)) of transient SEP at injection point within case 2 of the 1-layer earth model. The maximum peak value for the four curves is about 15.9 V. The resistivity of the earth is 100 Ωm and becomes smaller than 900 Ωm, and relative permittivity is also 10, which means that the mutual conductive effect becomes weaker, while mutual inductive and capacitive effects remain fixed. We note that once the mutual inductive effect has been neglected, the curve (c) of transient SEP at injection point becomes lower than the original curve (a). However, once the mutual capacitive effect has been neglected, the curve (b) of transient SEP at injection point is a superposition with the original curve (a). Meanwhile, the impulse impedances of the three cases are, respectively, $(2.94, 9.41 \times 10^{-5})\,\Omega$, $(2.92, 9.42 \times 10^{-5})\,\Omega$ and $(1.02, 5.94 \times 10^{-5})\,\Omega$. And once both mutual inductive and capacitive effects have been ignored, the impulse impedance become smaller as $(1.02, 5.94 \times 10^{-5})\,\Omega$, which is the same as the data produced with mutual inductive effect neglected. All these show that once mutual conductive effect becomes weaker due to lower resistivity of the earth, mutual inductive effects will become stronger. Meanwhile, mutual capacitive effects can be ignored.

Figure 2 also shows solid curves ((a), (b), (c), (d)) of transient SEP at injection point within case 3 of the 1-layer earth model. All parameters of the earth model are the same as those in case 2 earth model except that the relative permittivity is 80 instead of 10. Solid curves in Fig. 2 are almost the same as the dotted one in Fig. 2, and

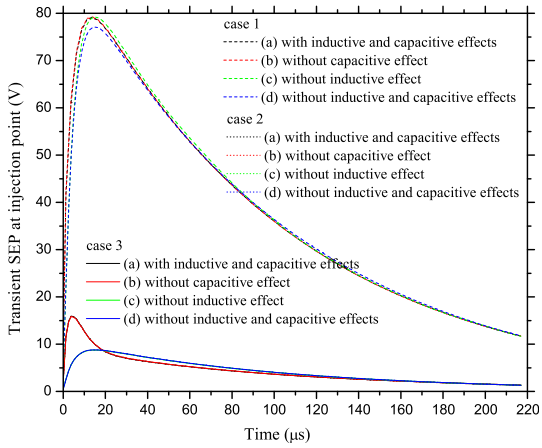

Figure 2. Transient SEP φ at the injection point within case 1, 2, 3 of the 1-layer earth model.

Table 2. Impulse impedances of case 1, 2, 3 of 1 layer earth model.

No.	case 1	case 2	case 3
a	$(9.23, 5.33 \times 10^{-4})$	$(2.94, 9.41 \times 10^{-5})$	$(2.94, 9.42 \times 10^{-5})$
b	$(9.24, 5.34 \times 10^{-4})$	$(2.92, 9.42 \times 10^{-5})$	$(2.92, 9.42 \times 10^{-5})$
c	$(9.21, 5.33 \times 10^{-4})$	$(1.02, 5.94 \times 10^{-5})$	$(1.02, 5.94 \times 10^{-5})$
d	$(8.91, 5.33 \times 10^{-4})$	$(1.02, 5.94 \times 10^{-5})$	$(1.02, 5.94 \times 10^{-5})$

all impulse impedances from case 3 in Fig. 2 are the same as that from case 2 in Fig. 2. All these show that the mutual capacitive effect can be ignored although the earth model owns larger relative permittivity .

Different from Fig. 2, Figs. 3 and 4 show frequency dependent characteristics of the real part of grounding impedance of grounding systems buried in the 1-layer earth model in frequency domain rather than time domain.

Figure 3 shows dashed curves ((e) black color, (f) red color, (g) green color, (h) blue color) of the real part of grounding impedance opposite to frequency within case 1 of 1-layer earth model. We can see that mutual capacitive effect is ignored, and the grounding impedance will increase with frequency increase, which can be seen in curve (f). Meanwhile, curve (f) is always lower than the original curve (e) with frequency increasing once frequency is above 0.1 MHz. However, once mutual inductive effect is ignored, the grounding impedance

will decrease with frequency increase, which can be seen in curve (g). Meanwhile, once both mutual capacitive and inductive effects are ignored, the grounding impedances are independent of frequency, which can be seen in line (h), and is always 8.30 Ω. All these show that for 1-layer earth model with high resistivity where grid is buried, the mutual inductive effect in frequency domain is much stronger than itself in time domain. Meanwhile, mutual capacitive effect in frequency is relatively stronger than itself in time domain.

Figure 3 also shows dotted curves ((e), (f), (g), (h)) of the real part of grounding impedance opposite to frequency within case 2 of the 1-layer earth model. We can see that mutual capacitive effect is ignored, and the grounding impedance will increase with frequency increase. We note that case 1 earth model owns high resistivity 900 Ωm. The curves ((e), (f)) do not superimpose once frequency is above 0.1 MHz in Fig. 3. However, here the resistivity becomes smaller, 100 Ωm. Curve (f) and original curve (e) are overlapped, which means that the mutual capacitive effects can be ignored. On the other hand, once mutual inductive effect is ignored, the grounding impedance will decrease with increase of frequency, which can be seen in curve (g). Meanwhile, once both mutual capacitive and inductive effects are ignored, the grounding impedance is independent of frequency (see line (h)) and is always 0.97 Ω. All these show that the mutual inductive effect is much stronger both in frequency and time domain within the low resistivity earth model; meanwhile, mutual capacitive effect can be ignored both in frequency and time domain within the low resistivity earth model

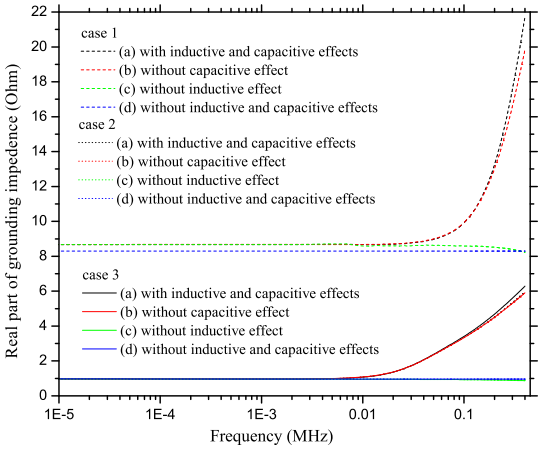

Figure 3. Real part of grounding impedance opposite to different frequencies within case 1, 2, 3 of the 1-layer earth model.

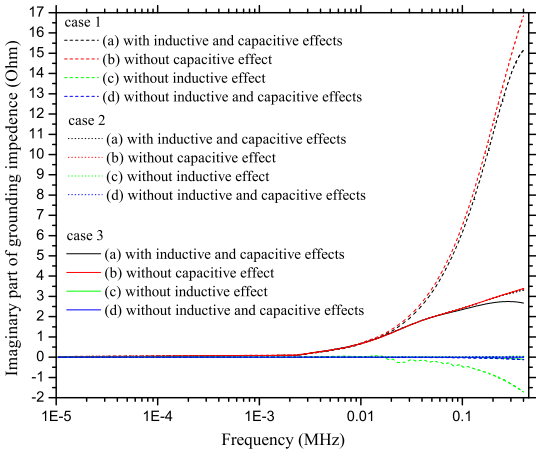

Figure 4. Imaginary part of grounding impedance opposite to different frequencies within case 1, 2, 3 of the 1-layer earth model.

with low relative permittivity.

Figure 3 also shows solid curves ((e), (f), (g), (h)) of the real part of grounding impedance opposite to frequency within case 3 of the 1-layer earth model. We can see that all solid curves are almost the same as the dotted one in Fig. 3. The only difference is that the curves ((e), (f)) do not be superimpose once frequency is above 0.05 MHz, which is produced by much bigger relative permittivity 80. All these show that the mutual capacitive effect in frequency domain is relatively stronger than itself in time domain within the low resistivity earth model with great relative permittivity.

Figure 4 shows frequency dependent characteristics of imaginary part grounding impedance of grounding systems, which are similar to the real part of one except the number of differences.

3.2. 2-layer Earth Model

The curves for transient SEP at injection point within three cases of 2-layer earth model are given in Fig. 5, and real and imaginary parts of grounding impedance within three cases of 2-layer earth model are given in Figs. 6, 7. Table 3 shows impulse impedances of the grounding system buried in the 2 layer earth model.

Figure 5 shows dashed curves ((a) black color, (b) red color, (c) green color, (d) blue color) of transient SEP at injection point within case 1 of 2-layer earth model. Compared with Fig. 2 for 1-layer earth model, all curves in Fig. 5 resemble the curves in Fig. 2.

However, the peak value for the four curves is about 52.3 V, smaller than the anterior peak value 78.8 V, because resistivity of second layer earth becomes smaller 500 Ωm instead of 900 Ωm, which brings much leakage currents into second layer earth while grounding grid is buried in first layer earth. All these show that all conclusions from 1-layer earth model are valid for 2-layer earth model with high resistivity.

Figure 5 also shows dotted curves ((a), (b), (c), (d)) of transient SEP at injection point within case 2 of the 2-layer earth model. Compared with Fig. 2 for 1-layer earth model, all curves in Fig. 5 resemble the curves in Fig. 2. However, the maximum peak value for the four curves is about 25.6 V, bigger than the anterior maximum peak value 15.9 V; meanwhile, the maximum peak value for the two curves produced without mutual inductive effect is about 21.3 V, bigger than the anterior maximum peak value produced without mutual inductive effect 8.84 V, because the resistivity of second layer earth becomes bigger 300 Ωm instead of 100 Ωm, which prevents much leakage currents

Table 3. Impulse impedances of case 1, 2, 3 of 2 layer earth model.

No.	case 1	case 2	case 3
a	$(6.08, 4.36 \times 10^{-4})$	$(4.73, 1.24 \times 10^{-4})$	$(4.74, 1.24 \times 10^{-4})$
b	$(6.10, 4.37 \times 10^{-4})$	$(4.72, 1.24 \times 10^{-4})$	$(4.72, 1.24 \times 10^{-4})$
c	$(5.92, 4.28 \times 10^{-4})$	$(2.47, 7.82 \times 10^{-5})$	$(2.47, 7.82 \times 10^{-5})$
d	$(5.77, 4.28 \times 10^{-4})$	$(2.45, 7.82 \times 10^{-5})$	$(2.45, 7.82 \times 10^{-5})$

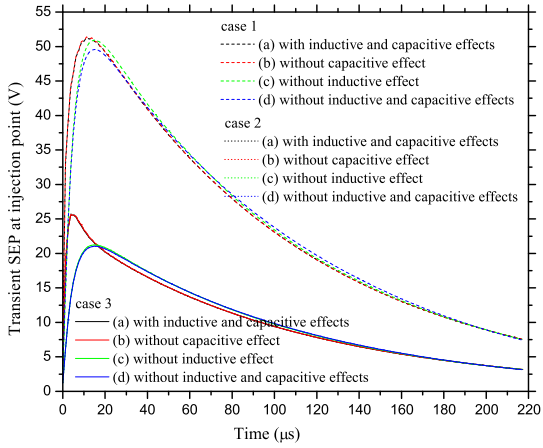

Figure 5. Transient SEP φ at the injection point within case 1, 2, 3 of the 2-layer earth model.

into second layer earth while grounding grid is buried in first layer earth. All these show that all conclusions from 1-layer earth model case are valid for 2-layer earth model with low resistivity.

Figure 5 also shows solid curves ((a), (b), (c), (d)) of transient SEP at injection point within case 3 of the 2-layer earth model, all parameters of the earth model are same as the one in case 2 of the 2-layer earth model except for all relative permittivities being 80 instead of 10. Solid curves in Fig. 5 are almost same as the dot one in Fig. 2 and all impulse impedances in Fig. 5 are same as the one in Fig. 2. All these show that the mutual capacitive effect can be ignored, which is same as the conclusion from 1-layer earth model case.

Different from Fig. 5, Figs. 6 and 7 will show frequency dependent characteristics of real part of grounding impedance of grounding systems buried in the horizontal 2-layer earth model.

Figure 6 shows dashed curves ((e) black color, (f) red color, (g) green color, (h) blue color) of the real part of grounding impedance opposite to frequency within case 1 of 2-layer earth model. Compared with Fig. 3 for 1-layer earth model, all curves in Fig. 6 resemble the curves in Fig. 3. We note that the grounding impedance 5.26 Ω being independent of frequency is smaller than foregoing 8.30 Ω, because second layer resistivity becomes smaller 500 Ωm instead of 900 Ωm. All conclusions from 1-layer earth model with high resistivity hold true for 2-layer earth model case.

Figure 6 shows dotted curves ((e), (f), (g), (h)) of the real part of grounding impedance opposite to frequency within case 2 of the

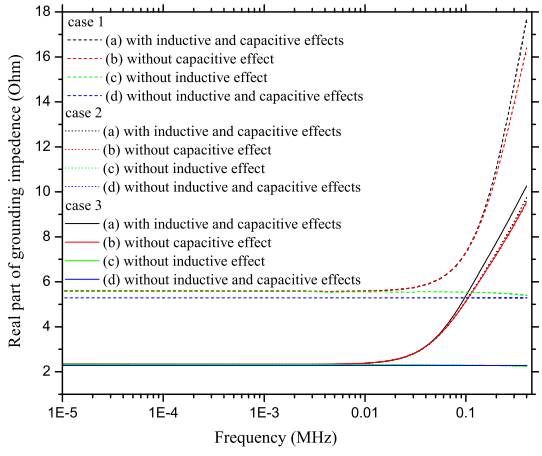

Figure 6. Real part of grounding impedance opposite to different frequencies within case 1, 2, 3 of the 2-layer earth model.

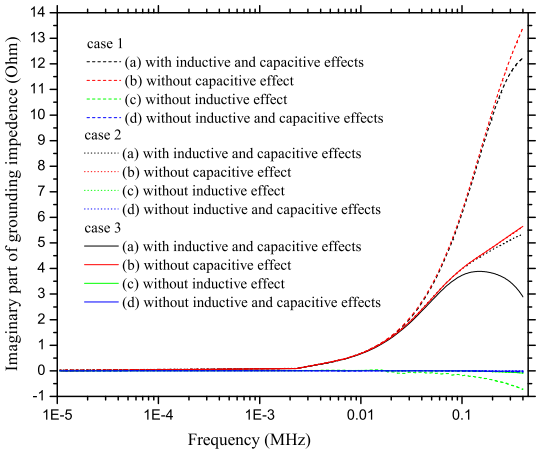

Figure 7. Imaginary part of grounding impedance opposite to different frequencies within case 1, 2, 3 of the 2-layer earth model.

2-layer earth model. Compared with Fig. 3 for 1-layer earth model, all curves in Fig. 6 resemble the curves in Fig. 3. We note that the grounding impedance 2.35 Ω being independent of frequency is bigger than foregoing 0.97 Ω, because second layer resistivity becomes bigger 300 Ωm instead of 100 Ωm. All conclusions from 1-layer earth model with low resistivity are howbeit valid for 2-layer earth model case.

Figure 6 shows solid curves ((e), (f), (g), (h)) of the real part of grounding impedance opposite to frequency within case 3 of the 2-layer earth model. Compared with Fig. 3 for 1-layer earth model, all solid curves in Fig. 6 resemble the dotted curves in Fig. 3. We know that all conclusions from 1-layer earth model with low resistivity and great relative permittivity are howbeit valid for 2-layer earth model case.

Figure 7 shows frequency dependent characteristics of imaginary part grounding impedance of grounding systems, like 1-layer earth case, which are also similarto the real part of one except the number of differences.

4. CONCLUSION

Combined with the FFT, maximal transient ground potential rise and frequency dependent impedance are analyzed in both time and frequency domains, respectively. Computations are done with a computer model based on the hybrid method. Results are presented which illustrate the properties of grounding systems to low as well as high frequency transients. For a general size of grounding grid, some

conclusions have be obtained by analyzing the numerical results as below:

(i) Frequency domain case: (1) For any earth model, the mutual inductive effect always has dominance, and cannot be neglected. (2) For an earth model with large relative permittivity (higher than 30), the mutual capacitive effect will be enhanced, but is always less than mutual inductive or conductive effect.

(ii) Time domain case: (1) For an earth model with high resistivity (higher than 300 Ωm), the mutual inductive effect can be ignored. (2) For an earth model with low resistivity (lower than 300 Ωm), the mutual inductive effect always has dominance and cannot be ignored. (3) For any earth model, the mutual capacitive effect can be ignored.

ACKNOWLEDGMENT

This work was funded by the Science and Technology Projects of State Grid Corporation of China under Contract Number: GY172011000JD and the National Natural Science Foundation of China under Grant 51177153.

REFERENCES

1. Grcev, L. and M. Heimbach, "Frequency dependent and transient characteristics of substation grounding system," *IEEE Transactions on Power Delivery*, Vol. 12, No. 1, 172–178, Jan. 1997.
2. Papalexopoulos, A. D. and A. P. Meliopoulos, "Frequency dependent characteristics of grounding systems," *IEEE Transactions on Power Delivery*, Vol. 2, No. 4, 1073–1081, Oct. 1987.
3. Huang, L. and D. G. kasten, "Model of ground grid and metallic conductor currents in high voltage a.c. substations for the computation of electromagnetic fields," *Electric Power Systems Research*, Vol. 59, 31–37, 2001.
4. Zhang, B., X. Cui, Z. B. Zhao, and J. L. He, "Numerical analysis of the influence between large grounding grids and two-end grounded cables by the moment method coupled with circuit equations," *IEEE Transactions on Power Delivery*, Vol. 20, No. 2, 731–737, 2005.
5. Takashime, T., T. Nakae, and R. Ishibashi, "High frequency characteristic of impedance to ground and field distributions of

ground electrodes," *IEEE Transactions on Power Apparatus and Systems*, Vol. 100, No. 4, 1893–1900, Apr. 1981.

6. Ramamoorty, M., M. M. B. Narayanan, S. Parameswaran, and D. Mukhedkar, "Transient performance of grounding grids," *IEEE Transactions on Power Delivery*, Vol. 4, No. 4, 2053–2059, Oct. 1989.
7. Liew, A. C. and M. Darveniza, "Dynamic model of impulse characteristics of concentrated earths," *Proc. Inst. Elect. Eng.*, Vol. 121, 123–135, Feb. 1974.
8. Wang, J., A. C. Liew, and M. Darveniza, "Extension of dynamic model of impulse behavior of concentrated grounds at high currents," *IEEE Transactions on Power Delivery*, Vol. 20, No. 3, 2160–2165, Jul. 2005.
9. Geri, A., "Behaviour of grounding systems excited by high impulse currents: The model and its validation," *IEEE Transactions on Power Delivery*, Vol. 14, No. 3, 1008–1017, Jul. 1999.
10. Devgan, S. S. and E. R. Whitehead, "Analytical models for distributed grounding systems," *IEEE Transactions on Power Apparatus and Systems*, Vol. 92, No. 5, 1763–1770, Sep./Oct. 1973.
11. Verma, R. and D. Mukhedkar, "Impulse impedance of buried ground wire," *IEEE Transactions on Power Apparatus and Systems*, Vol. 99, No. 5, 2003–2007, Sep./Oct. 1980.
12. Mazzetti, C. and G. M. Veca, "Impulse behavior of grounded electrodes," *IEEE Transactions on Power Apparatus and Systems*, Vol. 102, No. 9, 3148–3156, Sep. 1983.
13. Velazquez, R. and D. Mukhedkar, "Analytical modeling of grounding electrodes," *IEEE Transactions on Power Apparatus and Systems*, Vol. 103, No. 6, 1314–1322, Jun. 1984.
14. Menter, F. and L. Grcev, "EMTP-based model for grounding system analysis," *IEEE Transactions on Power Delivery*, Vol. 9, No. 4, 1838–1849, Oct. 1994.
15. Liu, Y., M. Zitnik, and R. Thottappillil, "An improved transmission-line model of grounding system," *IEEE Transactions on Electromagnetcs Compatibility*, Vol. 43, No. 3, 348–355, Aug. 2001.
16. Liu, Y., N. Theethayi, and R. Thottappillil, "An engineering model for transient analysis of grounding system under lightning strikes: Nonuniform transmission-line approach," *IEEE Transactions on Power Delivery*, Vol. 20, No. 2, 722–730, Apr. 2005.
17. Roubertou, D., J. Fontaine, J. P. Plumey, and A. Zeddam, "Harmonic input impedance of earth connections," *Proc. IEEE*

Int. Symp. Electromagnetic Compatibility, 717–720, 1984.

18. Dawalibi, F. and A. Selby, "Electromagnetic fields of enigized conductors," *IEEE Transactions on Power Delivery*, Vol. 8, No. 3, 1275–1284, Jul. 1986.
19. Grcev, L. and Z. Haznadar, "A novel technique of numerical modelling of impulse current distribution in grounding systems," *Proc. Int. Conf. on Lightning Protection*, 165–169, Graz, Austria, 1988.
20. Grcev, L. and F. Dawalibi, "An electromagnetic model for transients in grounding systems," *IEEE Transactions on Power Delivery*, Vol. 5, No. 4, 1773–1781, Oct. 1990.
21. Grcev, L., "Computation of transient voltages near complex grounding systems caused by lightning currents," *Proc. IEEE Int. Symp. Electromagnetic Compatibility*, 393–400, 1992.
22. Grcev, L., "Computer analysis of transient voltages in large grounding systems," *IEEE Transactions on Power Delivery*, Vol. 11, No. 2, 815-823, Apr. 1996.
23. Olsen, R. and M. C. Willis, "A comparison of exact and quasi-static methods for evaluating grounding systems at high frequencies," *IEEE Transactions on Power Delivery*, Vol. 11, No. 3, 1071–1081, Jul. 1996.
24. Poljak, D. and V. Doric, "Wire antenna model for transient analysis of simple grounding systems, part I: The vertical grounding electrode," *Progress In Electromagnetics Research*, Vol. 64, 149–166, 2006.
25. Poljak, D. and V. Doric, "Wire antenna model for transient analysis of simple grounding systems, part II: The horizontal grounding electrode," *Progress In Electromagnetics Research*, Vol. 64, 167–189, 2006.
26. Andolfato, R., L. Bernardi, and L. Fellin, "Aerial and grounding system analysis by the shifting complex images method," *IEEE Transactions on Power Delivery*, Vol. 15, No. 3, 1001–1010, Jul. 2000.
27. Dawalibi, F., "Electromagnetic fields generated by overhead and buried short conductors, part II-ground networks," *IEEE Transactions on Power Delivery*, Vol. 1, No. 4, 112–119, Oct. 1986.
28. Dawalibi, F. and R. D. Southy, "Analysis of electrical interference from power lines to gas pipelines, Part I, computation methods," *IEEE Transactions on Power Delivery*, Vol. 4, No. 3, 1840–1846, 1989.

29. Li, Z. X., W. J. Chen, J. B. Fan, and J. Y. Lu, "A novel mathematical modeling of grounding system buried in multilayer earth," *IEEE Transactions on Power Delivery*, Vol. 21, No. 3, 1267–1272, 2006.
30. Li, Z. X. and W. J. Chen, "Numerical simulation grounding system buried within horizontal multilayer earth in frequency domain," *Communications in Numerical Methods in Engineering*, Vol. 23, No. 1, 11–27, 2007.
31. Li, Z. X. and J. B. Fan, "Numerical calculation of grounding system in low frequency domain based on the boundary element method," *International Journal for Numerical Methods in Engineering*, Vol. 73, 685–705, 2008.
32. Li, Z. X., G. F. Li, J. B. Fan, and C. X. Zhang, "Numerical calculation of grounding system buried in vertical earth model in low frequency domain based on the boundary element method," *European Transactions on Electrical Power*, Vol. 19, No. 8, 1177–1190, 2009.
33. Otero, A. F., J. Cidras, and J. L. Alamo, "Frequency-dependent grounding system calculation by means of a conventional nodal analysis technology," *IEEE Transactions on Power Delivery*, Vol. 14, No. 3, 873–877, Jul. 1999.
34. Li, Z. X., G. F. Li, J. B. Fan and Y. Yin, "A novel mathematical model for the lightning response of a grounding system buried in multilayered earth based on the quasi-static complex image method," *European Transactions on Electrical Power*, Vol. 32, No. 1, 21–30, 2012.
35. Choma, J., *Electrical Networks — Theory and Analysis*, New York, 1985.
36. Stojkovic, Z., J. M. Nahman, D. Salamon, and B. Bukorovic, "Sensitivity analysis of experimentally determined grounding grid impulse characteristic," *IEEE Transactions on Power Delivery*, Vol. 13, No. 4, 1136–1143, Oct. 1998.